NASA CONTRACTOR REPORT

NASA CR-2179

ANALYSIS OF HIGH-ASPECT-RATIO JET-FLAP WINGS OF ARBITRARY GEOMETRY

by Peter B. S. Lissaman

Prepared by
NORTHROP CORPORATE LABORATORIES
Hawthorne, Calif. 90250
for Langley Research Center

NATIONAL AERONAUTICS AND SPACE ADMINISTRATION • WASHINGTON, D. C. • FEBRUARY 1973

1. Report No.	2. Government Accession No.	3. Recipient's Catalog No.
NASA CR-2179		

4. Title and Subtitle	5. Report Date
Analysis of High-Aspect-Ratio Jet-Flap Wings of Arbitrary Geometry	February 1973
	6. Performing Organization Code
7. Author(s)	8. Performing Organization Report No.
Peter B. S. Lissaman	
	10. Work Unit No.
9. Performing Organization Name and Address	
Northrop Corporate Laboratories 3801 West Broadway Hawthorne, California 90250	11. Contract or Grant No. NAS 1-10627
	13. Type of Report and Period Covered
12. Sponsoring Agency Name and Address	Contractor Report
National Aeronautics and Space Administration Washington, D. C. 20546	14. Sponsoring Agency Code

15. Supplementary Notes

16. Abstract

An analytical technique to compute the performance of an arbitrary jet-flapped wing is developed. The solution technique is based on the method of Maskell and Spence in which the well-known lifting-line approach is coupled with an auxiliary equation providing the extra function needed in jet-flap theory. The present method is generalized to handle straight, uncambered wings of arbitrary planform, twist, and blowing (including unsymmetrical cases). An analytical procedure is developed for continuous variations in the above geometric data with special functions to exactly treat discontinuities in any of the geometric and blowing data. A rational theory for the effect of finite wing thickness is introduced as well as simplified concepts of effective aspect ratio for rapid estimation of performance.

17. Key Words (Suggested by Author(s))	18. Distribution Statement
Jet flap, high-lift devices, lifting-line theory wing theory	Unclassified - Unlimited

19. Security Classif. (of this report)	20. Security Classif. (of this page)	21. No. of Pages	22. Price*
Unclassified	Unclassified	56	$3.00

*For sale by the National Technical Information Service, Springfield, Virginia 22151

ANALYSIS OF HIGH-ASPECT-RATIO JET-FLAP WINGS OF ARBITRARY GEOMETRY

By Peter B. S. Lissaman
Northrop Corporate Laboratories

SUMMARY

Many techniques of amplifying the lift of a wing involve the blowing of a thin, high energy sheet from the wing trailing edge (jet flap). Currently, no methods exist to rapidly compute the performance of an arbitrary jet-flapped wing.

This paper develops an analytical technique based on the method of Maskell and Spence in which the well-known lifting-line approach is coupled with an auxiliary equation providing the extra function needed in jet-flap theory. The method of Maskell and Spence was developed for a special class of wings of elliptical planform and loading. The present method generalizes this to handle straight, uncambered wings of arbitrary planform, twist, and blowing (including unsymmetrical cases). An analytical procedure is developed for continuous variations in the above geometric data with special functions to exactly treat discontinuities in any of the geometric and blowing data. A rational theory for the effect of finite wing thickness is introduced as well as simplified concepts of effective aspect ratio for rapidhand estimation of performance.

The procedure has been programed and prints out all relevant data. Each wing case takes less than six seconds on the CDC 6600.

The results converge properly to all known limit cases, and correlation with other known theoretical solutions for jet-flap wings is good. It is found that, although the method is a lifting-line technique, good accuracy was obtained for aspect ratios as low as 4. Correlation with experimental data was as good as other techniques, but it is pointed out that few properly controlled and corrected experimental tests are known.

It is believed that the accuracy of this method is quite adequate for jet-flap wing design and that the speed and flexibility of the program make it very suitable for preliminary design.

INTRODUCTION

Powered lift is becoming an increasingly important technique for STOL vehicles. In general, this consists of methods in which the energy of a certain mass of air is increased, and this mass then forced over aerodynamic surfaces to amplify the lifting effects. Typical examples of powered lift using a jet sheet with lifting-surface interaction are: jet-flap wing, externally blown flap, and augmentor wing. The theory developed in this analysis is applicable to all these types of lift amplification, since augmentor wings and externally blown flaps involve a similar analysis to jet-flap wings and may be approximated by thin sheet jet-flap theory.

The fluid dynamics of multi-energy flows is generally a poorly understood field. Although it is simple to write the basic equations satisfied at appropriate points, a full solution for a specified geometry is more difficult, even neglecting the effect of viscosity. In essence, this problem occurs because the unknown boundary between the two flows of different energy cannot be specified in advance. Since this boundary moves as the flow state is altered, the solutions are intrinsically nonlinear because of the nonlinear boundary conditions.

For the problem considered, a high energy jet sheet issuing from the trailing edge of the wing is assumed. The standard assumptions of incompressible inviscid flow, a thin jet, and linearized boundary conditions are made. This model is described in detail in reference 1.

SYMBOLS

a	intermediate complex mapping parameter
A	aspect ratio, $\frac{b^2}{S_w}$
A_e	effective aspect ratio (see eq. (59))
A_n	coefficients of Φ^c sine expansion
b	wing span, meters (ft)
c	local wing chord, meters (ft)
c'	chord of airfoil in auxiliary plane (app. B)
c^*	normalized chord, $\frac{c}{c_{av}}$
c_{av}	mean chord, $\frac{S_w}{b}$, meters (ft)
c_e	effective chord, (see eq. (19))
c_{ek}	effective chord at station, $\omega = \frac{k\pi}{r}$
c_j	momentum coefficient in auxiliary plane (app. B)
c_{j_1}	momentum coefficient in auxiliary plane at trailing edge (see eq. (B12))
C	chord of airfoil in physical plane, meters (ft) (see app. B)
C_ℓ	lift coefficient at a station

C_{ℓ_j} local lift coefficient due to jet momentum

C_{ℓ_p} two-dimensional normal pressure lift coefficient (see eq. (6))

C_{ℓ}^{t} two-dimensional lift coefficient finite thickness airfoil

C_{ℓ}^{o} two-dimensional lift coefficient zero thickness airfoil

C_{ℓ_α} two-dimensional lift coefficient gradient with angle of attack

C_{ℓ_θ} two-dimensional lift coefficient gradient with jet-flap deflection angle

C_d local induced-drag coefficient

C_{d_j} local induced-drag coefficient due to jet momentum

C_{d_p} local induced-drag coefficient due to pressure on airfoil

C_{D_I} wing-induced drag coefficient

C_j local jet-momentum coefficient, $\frac{\gamma}{\frac{1}{2}\rho V^2 c}$

C_J wing jet-momentum coefficient

C_L wing lift coefficient

C_{L_α} wing lift coefficient gradient with angle of attack

C_{L_θ} wing lift coefficient gradient with jet angle

C_{L_P} wing pressure lift coefficient

$C_{L_{P_\alpha}}$ wing pressure lift coefficient gradient with angle of attack

$C_{L_{P_\theta}}$ wing pressure lift coefficient gradient with jet angle

C_n local normal-force coefficient in airfoil

C_t local nose-thrust coefficient on airfoil

D induced drag of wing

E_{k_j} elements of matrix determining σ change

e induced drag efficiency

g(x) function used to define jump operator (see eq. (37))

f ratio of blown to unblown lift slope of airfoil (see eq. (59))

f* mapping derivative from physical to auxiliary plane

F_k elements of line vector denoting error in nose thrust

F_y, F_z components of force in Trefftz plane (app. A)

H Heaviside operator

J_{i_j}	elements of matrix defining discontinuous potential gradients
L	lift of wing, grams (lbs)
m,n,i,j	indices of summation
N	leading edge of airfoil (app. B)
N_o	nose source
N_{o_α}	gradient of nose source with angle of attack
N_{o_θ}	gradient of nose source with jet angle
q	complex conjugate velocity in auxiliary plane
q_∞	free-stream speed in auxiliary plane, meters/second (ft/sec)
Q	complex conjugate velocity in physical plane
Q_∞	free-stream speed in physical plane, meters/second (ft/sec)
r	even integer defining upper limit of potential function series, (see eq. (22))
R	radius of curvature of wake in physical plane
s	arc length in auxiliary plane (app. B)
S	arc length in physical plane (app. B)

S_w	wing area, meters^2 (ft^2)
t	thickness of airfoil in auxiliary plane (app. B)
T	thickness of airfoil in physical plane (app. B)
T'	trailing edge of airfoil (app. B)
V	main-stream velocity, meters/second (ft/sec)
w(z)	normalized complex perturbation potential in Trefftz plane
W	complex potential function
x	spanwise coordinate in Trefftz plane
X	spanwise coordinate normalized by semispan (2x/b)
y	vertical coordinate in Trefftz plane
Y	vertical coordinate normalized by semispan (2y/b)
z	complex coordinate in Trefftz plane (app. A)
z'	complex coordinate in auxiliary plane (app. B)
Z	complex coordinate in physical plane (app. B)
α	local wing angle of attack, radians
$\bar{\alpha}$	mean angle of wake in Trefftz plane, radians
α_e	effective angle of attack, radians (see eq. (20))

α_{e_k} effective angle of attack at station, $\omega = \frac{k\pi}{r}$, radians

α_i local induced angle of attack, radians

α_1 local effective angle of attack of jet-flap airfoil, radians, (see eq. (13))

α_2 local effective angle of attack of plain airfoil, radians

α_∞ local angle of downwash in Trefftz plane, radians

β local angle of jet wake in Trefftz plane, radians

β_{kn} elements of matrix defining potential gradient

$\beta_m^*(\omega)$ elements of line vector defining potential gradient at ω

$\beta_n^{**}(\omega_{d_j})$ elements of line vector used in discontinuous analysis

$\gamma(x)$ local jet-moment per unit span at station x

γ_a circulation about airfoil in auxiliary plane (app. B)

Γ circulation about airfoil and wake in physical plane, (app. B)

Γ_a circulation about airfoil alone in physical plane (app. B)

δ_{kn} Kronecker delta

Δp pressure perturbation in Trefftz plane (app. A)

ε	constant used in iteration technique (see eq. (47))
η	ratio of lift slope of thick unblown airfoil to zero thickness unblown airfoil (see eq. (54))
θ	local jet angle relative to chordline, radians
θ	slope of wake in auxiliary plane (app. B)
θ	slope of wake in physical plane (app. B)
λ_i	magnitude of i^{th} downwash discontinuity (see eq. (35))
μ	intermediate complex mapping parameter
ρ	density of main-stream flow, grams/meter^3 (slugs/ft^3)
σ	function relating Trefftz plane downwash to wing plane downwash
Φ	normalized potential function
Φ^c	continuous normalized potential function
Φ^*	discontinuous normalized potential function
ϕ_x, ϕ_y	gradient of potential function, w.r.t. x,y
χ_o	distance from leading edge of airfoil
ω	angular coordinate of wing station ($\cos^{-1} x$)
ω_{d_i}	angular coordinate of i^{th} discontinuity of wing geometry

PREVIOUS WORK

The linearized problem for the two-dimensional jet flap both in and out of ground effect has been treated in references 2 to 5. Excellent correlation of the theory with experiment has been found.

The three-dimensional problem has been handled by a number of workers using different approaches to handle the kinematic and dynamic boundary conditions in the wake. A semi-empirical method for computing wing performance is given by Kuchemann (ref. 6). Solutions using the techniques of matched asymptotic expansions have been published by Kerney (ref. 7) and Tokuda (ref. 8). All of these methods involve approximations about the wake location.

The model by Maskell and Spence (ref. 1) makes an attempt to handle the dynamic condition on the wake by using two-dimensional solutions which properly match the wake boundary conditions. However, this treats only the high-aspect-ratio elliptically loaded case. Perhaps the most advanced model is that given by Lopez and Shen (ref. 9). Although this model (like the others) is linearized, it utilizes lifting-surface theory, finding the wake deformation by iteration on the proper dynamic and kinematic boundary conditions.

The model proposed here lies somewhere between the method of Lopez and Shen (ref. 9) and that of Maskell and Spence (ref. 1) in its assumptions and complexity. It is essentially an extension of the blown lifting-line concept for a high-aspect-ratio wing of arbitrary planform and blowing. In the current model, methods are developed to take into account discontinuities in the wing geometry in chord, angle of attack, jet angle, or blowing coefficient.

ANALYSIS

General

The formal lifting-surface solution consists of matching kinematic boundary conditions on the wing as well as kinematic and dynamic boundary conditions on the loaded jet wake as shown by Lopez and Shen (ref. 9). An extension of the

Prandtl lifting-line approach as employed by Maskell and Spence (ref. 1) is adopted.

The basic idea (which may be formalized in terms of matched asymptotic expansions) is that the forces on the wing may be determined in two places. In the Trefftz plane, the forces may be uniquely determined in terms of wake parameters (essentially downwash and jet coefficient). On the wing itself (wing plane), the forces may be determined in terms of local section properties. Here, the main parameters are the blown airfoil characteristics and the induced downwash angle at the wing. The Trefftz plane and wing plane forces are then matched to provide sufficient equations for solution.

In the case of an unblown wing, the lift in the two planes is matched to provide a relationship between the potential ϕ and the Trefftz plane downwash ϕ_y generating the well-known integro-differential equation of lifting-line theory (Prandtl's equation). An important assumption is that the induced angle at the wing is taken to be half that in the Trefftz plane.

In the case of a blown wing, a major portion of the bound vorticity (that directly due to the jet sheet) is located downstream of the trailing edge. Thus, it is not valid to assume that the trailing vorticity emanates from a lifting-line situated within the wing chord.

The analysis involves only two space variables, with the coordinate system centered on the wing or wake centerline. The independent variable x is used for the spanwise dimension, positive towards the right wingtip where the wing is viewed from the rear, with y the vertical coordinate positive in the upwards (lift) direction. (See fig. 1.)

The approach of reference 1 is adopted and introduces a new constant σ (variable across the span) by which the Trefftz plane downwash is scaled. Thus, the downwash at the wing is assumed constant across each chordwise station and equal to $\sigma(x)\ \alpha_\infty(x)$ where $\alpha_\infty(x)$ is the downwash angle in the Trefftz plane. Hence, the induced angle $\alpha_i(x)$, as shown in figure 2, is given by

$$\alpha_i(x) = \sigma(x)\ \alpha_\infty(x) \qquad (1)$$

This implies that a further unknown is introduced into the wing plane solution, so that an additional matching equation is required. It seems natural then to match both the lift and drag equations, or equivalently, the normal and chordwise force equations providing the additional equation for σ. Reference 1 assumes that σ is constant across the span, as implied by the elliptical loading. In the present solution, σ is permitted to vary with x and determined at each spanwise station.

Trefftz Plane Solution

By considering the flow in the Trefftz plane and by resolving parallel and normal to the chord, a pair of equations is obtained for the normal pressure coefficient and the thrust coefficient on the wing. It should be noted that the total force on the wing constitutes the sum of the pressure force and the momentum force due to the jet. Since the latter can be directly computed from the kinematics, it is more convenient to work with the pressure forces alone. It is noted that all coefficients are normalized by division of the dimensional force by $1/2\ \rho\ V^2\ c$ for the two-dimensional quantities and by $1/2\ \rho\ V^2\ S_w$ for the integrated wing quantities, where ρ is the ambient density, V the free-stream velocity, c the local chord, and S_w the wing area. Appendix A shows these force coefficients to be given by

$$C_n = \frac{4\ \bar{\alpha}\ \phi}{c} - C_j\left(\bar{\alpha}\ \phi_y + \alpha + \theta\right) \tag{2}$$

$$C_t = \left(\frac{4\ \bar{\alpha}\ \phi}{c}\right)\left(\frac{\alpha + \bar{\alpha}\ \phi_y}{2}\right) + \frac{C_j}{2}\left\{\theta^2 - \left(\alpha + \alpha\ \phi_y\right)^2\right\} \tag{3}$$

Wing Plane Solution

This solution is required to relate the local wing angle of attack to its bound vorticity distribution. This distribution must be such that the downwash it causes when added to the trailing system flow produces the downwash necessary to match the physical kinematic boundary conditions on the wing (fig. 2).

Consistent with lifting-line theory, it is assumed that the local downwash may be computed by considering the downwash of a two-dimensional system as shown in reference 1. This solution must match the kinematic and dynamic boundary conditions appropriate to a jet-flapped airfoil.

There are two approximate approaches to the problem of defining the boundary vorticity. The first is to assume that the vorticity is composed of two parts - the one being that of a two-dimensional jet-flap airfoil at $\alpha_1 = \alpha - \alpha_\infty$ with a jet flap of strength C_j and angle θ (fig. 2). This gives a downwash field w_1. To satisfy the wing boundary condition, a further vorticity is required,and this is assumed to be that of a plain airfoil at α_2 giving downwash w_2. Thus, as shown in reference 1, the kinematic boundary condition on the wing is exactly satisfied, and the dynamic boundary condition on the wake approximately satisfied. The above model is called the alpha effective model.

An alternative approximation is to assume the vorticity is that corresponding to a two-dimensional jet-flap airfoil at the true effective angle $\alpha - \alpha_i$ but at a reduced jet strength. The new effective blowing coefficient C_{j_e} is obtained by maintaining the same momentum lift in the three-dimensional wing as in a two-dimensional jet-flap airfoil

$$C_j \left(\theta + \alpha - \alpha_\infty\right) = C_{j_e} \left(\theta + \alpha - \alpha_i\right) \tag{4}$$

This is called the C_j effective model.

Thus, the loss in jet effectiveness due to three-dimensional flow (essentially involving the downwash due to the trailing vortex field) may be accounted for either by a reduced effective angle of attack or by a reduced effective momentum coefficient.

Combination of Trefftz and Wing Equations

It has been shown that introducing σ as an unknown requires two Trefftz and wing equations to close the set. The Trefftz plane solution gives unambiguous results for C_n and C_t. The wing plane gives two alternative

expressions for C_n and C_t. Thus, in principle, these are four consistent sets which could be chosen. For our purposes, the α effective assumption was selected for both C_n and C_t since this is slightly simpler algebraically.

Coefficients Using α Assumption

For this model, the lift coefficient due to the jet-flap airfoil at α_1, θ is $C_{\ell_\alpha} \alpha_1 + C_{\ell_\theta} \theta$ (where C_{ℓ_α} and C_{ℓ_θ} are the lift slopes for the jet-flap airfoil at the appropriate C_j). Expressions for C_{ℓ_α} and C_{ℓ_θ} are given in reference 2. In addition, there is the lift due to the plain wing vorticity of a flat plate at α_2, $2\pi \alpha_2$. Thus, the lift coefficient is

$$C_\ell = 2\pi \alpha_2 + C_{\ell_\alpha} \alpha_1 + C_{\ell_\theta} \theta \tag{5}$$

Subtracting the jet momentum $C_j (\alpha_1 + \theta)$ in order to obtain the normal pressure lift coefficient gives

$$C_{\ell_p} = 2\pi \alpha_2 + \left(C_{\ell_\alpha} - C_j\right) \alpha_1 + \left(C_{\ell_\theta} - C_j\right) \theta \tag{6}$$

For the nose thrust, the singular behavior near the leading edge is required. This may be represented in the form of a nose source N_o as described in reference 5 such that the perturbation near the nose behaves like $N_o/\chi_o^{1/2}$ where χ_o is the distance from the leading edge. It is shown in reference 5 that this can be written for a two-dimensional jet flap as

$$N_o = N_{o_\alpha} \alpha + N_{o_\theta} \theta \tag{7}$$

For the plain airfoil vorticity, $N_{o_\alpha} = 1.0$. Thus, the total nose singularity constant is given by

$$N_o = N_{o_\alpha} \alpha_1 + \alpha_2 + N_{o_\theta} \theta \tag{8}$$

As shown in reference 5, this singularity accounts entirely for the nose thrust which is given by

$$C_t = 2\pi\left(N_{o_\alpha}\,\alpha_1 + \alpha_2 + N_{o_\alpha}\,\theta\right)^2 \tag{9}$$

Jet-flap theory (ref. 5) gives

$$N_{o_\alpha}{}^2 = \left(\frac{2\,C_{\ell_\alpha} - C_j}{4\pi}\right) \tag{10}$$

$$N_{o_\theta}{}^2 = \frac{C_j}{4\pi} \tag{11}$$

These expressions may now be coupled with the results from the outer solutions.

Coupling

Combining the Trefftz and Wing solutions (eqs. (2) and (6)) for the pressure lift coefficients gives

$$\frac{4\,\bar{\alpha}\,\phi}{c} - C_j\left(\bar{\alpha}\,\phi_y + \alpha + \theta\right) = 2\pi\,\alpha_2 + \left(C_{\ell_\alpha} - C_j\right)\alpha_1 + \left(C_{\ell_\theta} - C_j\right)\theta \tag{12}$$

Substituting the geometrical results

$$\alpha_i = \alpha - \alpha_\infty = \alpha + \bar{\alpha}\,\phi_y \tag{13}$$

and

$$\alpha_1 = \sigma\,\alpha_\infty \tag{13a}$$

results in

$$\frac{4\,\phi\,\bar{\alpha}}{c} = 2\pi\left(\sigma - 1\right)\bar{\alpha}\,\phi_y + C_{\ell_\alpha}\left(\alpha + \bar{\alpha}\,\phi_y\right) + C_{\ell_\theta}\,\theta \tag{14}$$

Applying the same procedure to the thrust equations (eqs. (3) and (9)) gives

$$2\pi \left\{ N_{o_\alpha} \left(\alpha + \bar{\alpha}\, \phi_y\right) + N_{o_\theta}\, \theta + \bar{\alpha}\, \phi_y \left(1 - \sigma\right) \right\}^2 =$$

$$\left(\frac{4\, \bar{\alpha}\, \phi}{c}\right) \left(\frac{\alpha + \bar{\alpha}\, \phi_y}{2}\right) + \left(\frac{C_j}{2}\right) \left\{ \theta^2 - \left(\alpha + \bar{\alpha}\, \phi_y\right)^2 \right\} \tag{15}$$

Relationship With Prandtl Equation

It should be noted that equation (12) is actually an equation connecting ϕ and ϕ_y and represents the boundary conditions on the harmonic function ϕ. These boundary conditions are known as Riemann-Hilbert-Poincare conditions; where one part of a harmonic function is defined as a function of derivatives of its conjugate. In order to transform this into the classical integro-differential form, it is only necessary to note that

$$\phi_y = \frac{1}{2\pi} \int_{-b/2}^{b/2} \frac{\phi_x}{t - x}\, dt \tag{16}$$

by the harmonic property of ϕ. Noting that ϕ is proportional to the circulation Γ, this is recognized as the classical downwash integral of lifting-line theory. Thus, the equation representing the boundary relationship between ϕ and ϕ_y coupled with the harmonic property of ϕ will always give rise to an integro-differential equation relating ϕ and $\int (\phi_x/t - x)\, dt$.

SOLUTION TECHNIQUE

General

The method employed is to assume a σ distribution and use collocation methods to solve equation (12). Then the results of this solution are substituted into equation (15), and a new result for σ is obtained.

Normalization of Lift Equation

Equation (12) can be rewritten in the form

$$\frac{4\,\bar{\alpha}\,\phi}{c\left\{C_{\ell_\alpha} - 2\pi\,(1-\sigma)\right\}} = \frac{C_{\ell_\alpha}\,\alpha + C_{\ell_\theta}\,\theta}{\left\{C_{\ell_\alpha} - 2\pi\,(1-\sigma)\right\}} + \bar{\alpha}\,\phi_y \tag{17}$$

Putting $Y = 2y/b$, $X = 2x/b$, $c^* = c/c_{av}$, $c_{av} = S_w/b$, $A = b/c_{av}$, and $\Phi = \bar{\alpha}\phi/c_{av}$ where b is the wing span , S_w the area , and c_{av} the mean chord gives

$$\frac{4\,\Phi}{c^*\left\{C_{\ell_\alpha} - 2\pi\,(1-\sigma)\right\}} = \frac{C_{\ell_\alpha}\,\alpha + C_{\ell_\theta}\,\theta}{\left\{C_{\ell_\alpha} - 2\pi\,(1-\sigma)\right\}} + \frac{2}{A}\,\Phi_Y \tag{18}$$

This has the same form as the Prandtl equation for a plain wing of lift slope 2π, euiivalent chord c_e , and twist α_e , where

$$c_e = 2\,c^*\left\{\frac{C_{\ell_\alpha}}{2\pi} - (1-\sigma)\right\} \tag{19}$$

$$\alpha_e = \frac{C_{\ell_\alpha}\,\alpha + C_{\ell_\theta}\,\theta}{4\pi\left\{\frac{C_{\ell_\alpha}}{2\pi} - (1-\sigma)\right\}} \tag{20}$$

so that equation (18) becomes

$$\frac{4\Phi}{\pi\,c_e} = 2\,\alpha_e + \frac{2}{A}\,\Phi_Y \tag{21}$$

Potential Functions

Continuous potential. - Writing the spanwise coordinate $X = \cos\omega$, the continuous potential Φ^c can be defined as

$$\Phi^c = \sum_{n=1}^{r-1} A_n \sin n\omega \tag{22}$$

$$\Phi_Y^c = \frac{1}{\sin \omega} \sum_{n=1}^{r-1} n A_n \sin n\omega \tag{23}$$

It can be shown for r even (ref. 10) if Φ_m^c is defined at the pivotal points $\omega = m\pi/r$ with

$$\Phi_m^c = \frac{1}{\sin \omega} \sum_{n=1}^{r-1} A_n \sin n \frac{m\pi}{r} \tag{24}$$

that the gradient Φ_Y^c can be written at each pivotal point as

$$\Phi_Y^c(k) = \sum_{n=1}^{r-1} \Phi_n^c \beta_{kn} \tag{25}$$

where

$$\beta_{kn} = \frac{1}{r \sin \frac{n\pi}{r}} \left\{ \frac{1}{1 - \cos \frac{(n+k)\pi}{r}} - \frac{1}{1 - \cos \frac{(n-k)\pi}{r}} \right\}$$

for $k \pm n$ odd (26a)

$$= \frac{r}{\left(2 \sin \frac{n\pi}{r}\right)} \quad \text{for } k = n \tag{26b}$$

$$= 0 \quad \text{for } k \pm n \text{ even}, k \neq n \tag{26c}$$

Thus, if a continuous distribution is considered only and equation (21) satisfied at the pivotal points, the following is obtained

$$\sum_{n=1}^{r-1} \left(\frac{2}{A} \beta_{kn} + \frac{4}{\pi\, c_e(k)} \delta_{kn} \right) \Phi_n^c = 2\, \alpha_e(k) \tag{27}$$

where

$$\delta_{kn} = 1 \quad k = n \tag{28a}$$

$$\delta_{kn} = 0 \quad k \neq n \tag{28b}$$

It is sometimes convenient to compute the potential gradient at other than the pivotal point. It can be shown that this is given by

$$-\Phi_\gamma^c(\omega) = \sum_{n=1}^{r-1} \Phi_m^c\, \beta_m^*(\omega) \tag{29}$$

where

$$\beta_m^*(\omega) = \frac{1}{4\, r \sin \omega}$$

$$\left\{ \frac{(r-1)\cos\left\{ r\left(\omega - \frac{m\pi}{r}\right)\right\} - r\cos\left\{(r-1)\left(\omega - \frac{m\pi}{r}\right)\right\} + 1}{\cos\left(\omega - \frac{m\pi}{r}\right) - 1} \right.$$

$$\left. - \frac{(r-1)\cos\left\{ r\left(\omega + \frac{m\pi}{r}\right)\right\} - r\cos\left\{(r-1)\left(\omega + \frac{m\pi}{r}\right)\right\} + 1}{\cos\left(\omega + \frac{m\pi}{r}\right) - 1} \right\} \tag{30}$$

Discontinuous potential. - For discontinuous wing geometry, it is necessary to have a potential function which is continuous, with the proper behavior at the wingtips and at infinity and which has a finite jump in its derivative $\Phi_{i\gamma}$ at a given station ω_{d_i}. The function Φ_i^* which satisfies this has the property

$$\Phi_i^* (\omega) = \frac{1}{\pi}\left[\left(\cos\omega - \cos\omega_{d_i}\right) 1 \left\{\frac{\sin\left(\frac{\omega + \omega_{d_i}}{2}\right)}{\sin\left(\frac{\omega - \omega_{d_i}}{2}\right)}\right\} + \omega_{d_i} \sin\omega\right] \tag{31}$$

$$\Phi_{i_\gamma}^* (\omega) = - H\left(\omega_{d_i} - \omega\right) \tag{32}$$

where H is the Heaviside function with the property

$$H\left(\omega_{d_i} - \omega\right) = 1 \quad \text{for} \quad \omega \leq \omega_d \tag{33}$$

$$H\left(\omega_{d_i} - \omega\right) = 0 \quad \text{for} \quad \omega > \omega_d \tag{34}$$

It can be seen in the analysis that this function is capable of exactly matching a discontinuity in either c_e or α_e at ω_d.

General discontinuous solution. - It can be assumed that discontinuities in effective geometric data (c_e and α_e) occur at s points, given by ω_{d_i}, $i = 1 \ldots s$. Then the general potential can be written in the form

$$\Phi (\omega) = \sum_{n=1}^{r-1} A_n \sin n\omega + \sum_{i=1}^{s} \lambda_i \Phi_i^* (\omega) \tag{35}$$

where λ_i is the magnitude of the i^{th} discontinuity in downwash.

Now substituting into the general normalized lift (eq. (21)) at the pivotal points, this gives

$$\sum_{n=1}^{r-1} \left(\frac{2}{A} \beta_{kn} + \frac{4}{\pi c_e} \delta_{kn} \right) \Phi_n^c +$$

$$+ \sum_{i=1}^{s} \left\{ \frac{2}{A} H\left(\omega_{d_i} - \frac{k\pi}{r}\right) + \frac{4}{\pi c_{e_k}} \Phi_i^* \left(\frac{k\pi}{r}\right) \right\} \lambda_i = 2 \alpha_{e_k}$$

$$k = 1 \cdots r - 1 \qquad (36)$$

where c_{e_k} is the equivalent chord c_e at the kth pivotal point and similarly with α_{e_k}.

This yields $r - 1$ linear equations for the $r - 1 + s$ unknowns, Φ_n and λ_i. The additional s equations are obtained by considering the jump condition at each discontinuity.

Jump Condition

The jump operator $|_d$ on the function $g(x)$ can be defined in the following way

$$g(x) |_d = \operatorname*{Lim}_{\delta \to 0} \left\{ g(d) - g(d + \delta) \right\} \qquad (37)$$

Equation (35) can be written

$$\frac{4}{\pi} \Phi^c(\omega) + \frac{4}{\pi} \sum_{i=1}^{s} \lambda_i \Phi_i^*(\omega) = 2 \alpha_e c_e - \frac{2}{A} c_e \sum_{n=1}^{r-1} \Phi_n^c \beta_n^*(\omega)$$

$$- \frac{2}{A} c_e \sum_{i=1}^{s} \lambda_i H\left(\omega_{d_i} - \omega\right) \qquad (38)$$

The jump operator is now applied at each discontinuity. Then, noting that Φ^c and Φ^* are continuous throughout, this gives

$$0 = 2\,\alpha_e\,c_e\,|_{\omega_{d_j}} - \frac{2}{A}\,c_e\,|_{\omega_{d_j}} \sum_{n=1}^{r-1} \Phi_n^c\,\beta_n^*\left(\omega_{d_j}\right) - \frac{2}{A}\left\{c_e \sum_{i=1}^{s} \lambda_i\,H\left(\omega_{d_i} - \omega_{d_j}\right)\right\}|_{\omega_{d_j}} \quad .. \; j = 1 \,..\, s \tag{39}$$

Now, defining

$$\Delta(\alpha_e\,c_e)_j = (\alpha_e\,c_e)\,|_{\omega_{d_j}} \qquad j = 1 \cdots s \tag{40}$$

$$J_{ij} = \left\{c_e\,H\left(\omega_{d_i} - \omega_{d_j}\right)\right\}|_{\omega_{d_i}} \qquad \begin{matrix} j = 1 \cdots s \\ i = 1 \cdots s \end{matrix} \tag{41}$$

$$\beta_n^{**}\left(\omega_{d_j}\right) = \left\{\beta_n^*\left(\omega_{d_j}\right) c_e\right\}|_{\omega_{d_j}} \qquad \begin{matrix} j = 1 \cdots s \\ n = 1 \cdots r-1 \end{matrix} \tag{42}$$

the set obtained is

$$\sum_{n=1}^{r-1} \beta_n^{**}\left(\omega_{d_j}\right) \Phi_n^c + \sum_{i=1}^{s} J_{ij}\,\lambda_i = A\,\Delta\left(\alpha_e\,c_e\right)_j \qquad j = 1 \cdots s \tag{43}$$

This provides the remaining s linear equations. Equations (36) and (43) are then inverted for the solutions Φ_n^c and λ_i. From these, the potential may be evaluated by substituting into equation (35).

Auxiliary Thrust Equation

Once the potential has been determined for the first assumed σ distribution, the thrust equation is checked, and a multidimensional Newton's method used to establish the variation of the thrust equation with σ .

The thrust coefficient at the wing plane is given in normalized form from equation (15) as

$$C_t^W = 2\pi \left\{ N_{o_\alpha} \left(\alpha + \frac{2\,\Phi_\gamma}{A} \right) + N_{o_\theta}\, \theta - 2\,\Phi_\gamma \left(\frac{1 - \sigma}{A} \right) \right\}^2 \tag{44}$$

In the Trefftz plane, the thrust coefficient can be given by the right-hand side of equation (15) as

$$C_t^t = \frac{4\,\Phi \left(\alpha + \frac{\Phi_\gamma}{A} \right)}{c^*} + C_j \frac{\left\{ \theta^2 - \left(\alpha + \frac{2\,\Phi_\gamma}{A} \right)^2 \right\}}{2} \tag{45}$$

At each pivotal point or singular point, the error function F_K is

$$F_k = C_t^t\,(k) - C_t^W\,(k) \qquad k = 1 \cdots r - 1 + s \tag{46}$$

Then, σ at each point can be varied by a fixed value ε , generating a matrix

$$E_{kj} = \left(\frac{F_k \left(\sigma_j + \varepsilon \right) - F_k \left(\sigma_j \right)}{\varepsilon} \right) \qquad \begin{matrix} k = 1 \cdots r - 1 + s \\ j = 1 \cdots r - 1 + s \end{matrix} \tag{47}$$

The change in σ and $\Delta\sigma_j$ required to make F_k zero is now given by

$$\Delta\sigma_j = - \left(E_{kj} \right)^{-1} F_k \tag{48}$$

NUMERICS AND ITERATION PROCESS

General

The procedure used is to solve equations (36) and (43) for $\sigma = 0.5$, then to substitute the values of Φ into the auxiliary thrust equation (48) to determine a new set of σ values to insert in equations (36) and (43) and to continue this process until the maximum change in σ is less than an arbitrary assigned value.

The program was written with the capacity to handle 8 points of discontinuity and 21 pivotal points. The only numerical constants required are the blown-lift coefficient slopes. This analysis uses the results given in reference 1:

$$C_{\ell_\alpha} = 2\pi \left(1 + 0.151\ C_j^{1/2} + 0.291\ C_j\right) \tag{49}$$

$$C_{\ell_\theta} = 2\left(\pi\ C_j\right)^{1/2} \left(1 + 0.151\ C_j^{1/2} + 0.139\ C_j\right)^{1/2} \tag{50}$$

It was found that only four iterations were required to bring the interative changes σ down to 10^{-5} so that convergence in all cases was very rapid. Programed on the CDC 6600, a given wing planform takes less than 2 seconds to run. The program is written with attention to divisors, so that the case $C_j = 0$ can be treated directly. Thus, plain unblown discontinuous wings may also be handled by the program.

Local Integral Properties

Three items of interest are the local lift, induced angle at infinity, and induced drag. If Φ is the solution, it can readily be shown that

$$C_\ell = \frac{4\ \Phi}{c^*} - 2\ C_j\ \frac{\Phi_Y}{A} \tag{51}$$

$$\alpha_\infty = -\ 2\ \frac{\Phi_Y}{A} \tag{52}$$

$$C_{d_i} = C_\ell\ \frac{\alpha_\infty}{2} \tag{53}$$

These coefficients can be integrated across the span (taking due account of singularities) to give the integral wing properties C_L and C_{D_I}.

THICKNESS EFFECT

The preceding analysis is done for airfoils of zero thickness. The thickness effect can approximately be incorporated by using a modified lift slope in the wing-plane equation, as is normally done in the lifting-line approach to wing theory.

On this basis, the lift slope of a plain wing of finite thickness can be written as $2\pi\eta$ and that of the jet-flap wing of thickness t as $C^t_{\ell_\alpha}$ and $C^t_{\ell_\theta}$. Expressions for the latter quantities are derived in Appendix B. Substituting these modified lift slopes into the wing-plane lift equation, it can be found that the equivalent chord and angle of attack (eqs. (19) and (20)) become

$$c_e = 2\,c^* \left\{ \frac{C_{\ell_\alpha}}{2\pi} - \eta\left(1 - \sigma\right) \right\} \tag{54}$$

$$\alpha_e = \frac{C^t_{\ell_\alpha}\,\alpha + C^t_{\ell_\theta}\,\theta}{4\pi\left\{ \frac{C^t_{\ell_\alpha}}{2\pi} - \eta\left(1 - \sigma\right) \right\}} \tag{55}$$

With these new definitions, equation (21) is unchanged.

EFFECTIVE ASPECT RATIO

Aspect ratio plays a dominant role as the scaling parameter in the lifting-line equation since the solution depends in a continuous, but nonlinear, fashion upon aspect ratio.

For blown wings, the significance of the geometrical aspect ratio is obscured by the additional parameters C_J and θ. However, it can be shown that, for an elliptically loaded blown wing, an equivalent aspect ratio can be defined which has many useful properties.

The basic integral equation for the jet-flap wing is

$$\frac{4\,\Phi}{\pi\,c^*} = 2\,\frac{C_{\ell_\alpha}\,\alpha + C_{\ell_\theta}\,\theta}{2\pi} + \frac{2}{A}\,\frac{C_{\ell_\alpha} - 2\pi\,(1-\sigma)}{\pi}\,\Phi_\gamma \tag{56}$$

Differentiation with respect to α gives

$$\frac{4\,\Phi_\alpha}{\pi\,c^*} = \frac{C_{\ell_\alpha}}{\pi} + \frac{2}{A\,\pi}\left\{C_{\ell_\alpha} - 2\pi\,(1-\sigma)\right\}\Phi_{\alpha\gamma} \tag{57}$$

An unblown wing, where $\sigma = 1/2$ and $C_{\ell_\alpha} = 2\pi$, gives

$$\frac{4\,\Phi_\alpha}{\pi\,c^*} = 2 + \frac{2}{A}\,\Phi_{\alpha\gamma} \tag{58}$$

If

$$f = \frac{C_{\ell_\alpha}}{2\,\pi} \tag{59}$$

and

$$A_e = \frac{A}{2\left\{f - (1-\sigma)\right\}} \tag{60}$$

equation (57) becomes

$$\frac{4\,\Phi_\alpha}{\pi\,f\,c^*} = 2 + \frac{2\,\Phi_{\alpha\gamma}}{f\,A_e} \tag{61}$$

This converts equations (57) and (58) into identical equations. If f and σ are not functions of spanwise position, equation (61) can be solved by using standard theory for an unblown wing of aspect ratio A_e.

For the elliptically loaded case, this assumption of spanwise invariance is valid and f can be determined from two-dimensional jet-flap theory. However, σ cannot be determined without an auxiliary equation. Assuming σ is known, where C_L is the mean wing-lift coefficient, equation (61) can be solved to obtain

$$C_{L_\alpha} = f\left\{\frac{2\pi}{1 + \frac{2}{A_e}}\right\}\left\{\frac{1 + 2\,C_J}{\pi\ A_e}\right\} \tag{62}$$

giving

$$\frac{C_{L_\alpha}}{C_{\ell_\alpha}} = \frac{1}{1 + \frac{2}{A_e}}\left\{1 + \frac{2\,C_J}{\pi\ A_e}\right\} \tag{63}$$

where C_{ℓ_α} is the two-dimensional lift slope. A similar result can be shown for C_{L_θ}. Thus, the interesting general result that can be obtained is

$$\frac{C_L}{C_\ell} = \frac{1}{\left(1 + \frac{2}{A_e}\right)} \cdot \left\{1 + \frac{2\,C_J}{\pi\ A_e}\right\} \tag{64}$$

This result is true for all elliptically loaded high-aspect-ratio wings - blown or unblown. The induced drag may also be written (exactly for an elliptically loaded wing) as

$$C_{D_I} = \frac{C_L{}^2}{\pi\ A + C_J} \tag{65}$$

For a wing of arbitrary loading, f and σ will in general vary across the span; however, these equations will be approximately valid for some mean values of $\bar{f}$ and $\bar{\sigma}$ and can be written as

$$\frac{C_L}{C_\ell} = \frac{1}{1 + \frac{2}{A_e}}\left\{1 + \frac{2\,C_J}{\pi\,A_e}\right\} \tag{66}$$

$$C_{D_I} = \frac{C_L{}^2}{e\left(\pi\,A + 2\,C_J\right)} \tag{67}$$

where

$$A_e = A\left[2\left\{\bar{f} - (1 - \bar{\sigma})\right\}\right] \tag{68}$$

and e is an induced-drag efficiency which will be less than unity.

It should be noted in this representation σ must be known and cannot, in fact, be determined without solving the lift and thrust equations. However, these results can be useful if an estimate for $\bar{\sigma}$ is known from previous experience.

RESULTS AND COMPARISON WITH THEORY AND EXPERIMENT

Check of Analysis

It should be noted that the various known limit cases are corre tly obtained with this model. Putting the aspect ratio equal to infinity recovers the proper two-dimensional jet-flap airfoil performance. For elliptical loading, a constant σ across the span is obtained with uniform downwash and lift coefficients. For zero blowing, the proper lifting-line solution for the wing is obtained. The discontinuous input was found to check with results given in reference 10 for an unblown wing with twist discontinuities.

A severe test of the discontinuity analysis was made by taking an inverse problem as a test case. Here, a uniform downwash was assumed, implying an ellipticaly loading. However, the wing planform was given a chordwise discontinuity with the elliptical loading maintained by appropriate discontinuities in angle of attack. This particular discontinuous geometry was used as input into the direct

program which then inverted to the integral equation to recover the uniform downwash and elliptical loading to the fourth significant place.

A check of linearity was made by determining the lift slope for a set of increasing angles of attack from 1° to 30°. It was found that the slope remained the same to the fourth significant place. This is interesting in view of the fact that, although the lift equation is properly linear, the auxiliary equation for σ is actually quadratic in α.

Basic Results

There is such a large set of results available from the program that it is of no particular value to display wing performance for some arbitrary set of geometries. The elliptical cases have already been given in reference 1. Thus, for design purposes, the next most generally significant wing could be considered to be the constant-chord straight wing with constant spanwise blowing. A series of results for varying aspect-ratio and blowing coefficients are shown in figure 3 for rectangular wings of 0-percent thickness.

It is convenient here to plot only the pressure-lift coefficient; that is, the wing-system lift after the jet-momentum contribution has been subtracted. Typically, at a station, the pressure-lift coefficient is given by

$$C_{\ell_p} = C_\ell - C_j\,(\theta + \alpha) \tag{69}$$

while the wing-pressure-lift coefficient is given by

$$C_{L_p} = \frac{1}{S}\int C_{\ell_p}\, c\, db \tag{70}$$

It should be noted that C_{L_p} is really the significant term in any evaluation of the solution technique, since the momentum lift may be mechanically and exactly computed for any planform. By removing the momentum lift, any differences in the solution approach may be more clearly identified. Because of the linearity of the

analysis, the results are further condensed by considering only the gradients with α and θ - that is, $C_{L_{p_\alpha}}$ and $C_{L_{p_\theta}}$. It can be seen from figure 3 that this results in a fairly compact presentation of performance. It is also noteworthy, that for blowing coefficients above 4, there is little variation in the lift slopes with increasing C_j.

The thickness effect is very significant. For an unblown wing of constant thickness, it can be shown that the thickness term can be accounted for by writing $2\pi\eta$ as the section lift slope; then, the lift slope of the thick wing becomes η multiplied by the lift slope of a 0-percent-thick wing of aspect ratio A/η. The effect is to increase the three-dimensional lift slope by an amount somewhat less than η. A similar effect occurs for the blown wing; however, this appears to be rather large when referred to pressure lift. Figure 4 shows a comparison of pressure-lift slopes for 0-percent-thick and 10-percent-thick wings. It can be seen that the thickness is as significant as aspect ratio in determining performance. This point becomes important in comparing the theory with analytical results.

The generalized induced drag efficiency e (eq. (67)) is a useful quantity. since this indicates how well a given wing approaches its minimum blown induced drag. For rectangular wings, these values of e are shown in figure 5. It can be seen that the efficiency values are quite high and suggest that for uniform blowing the induced drag of rectangular wings can be approximated by the well-known elliptical blown induced-drag expression.

Comparison With Other Theories

It should be noted first that since the analysis is an approximation to the actual lifting-surface model, which is itself an idealized model of the actual flow, the theoretical comparison of existing approaches should initially be discussed. The present paper is a lifting-line analysis and, in this respect, is similar to those by Maskell and Spence (ref. 1), Kerney (ref. 2), Tokuda (ref. 8), and the section design method of Lopez and Shen (ref. 9). The latter three methods do not use an auxiliary equation to determine σ, but assume it has its unblown value of one half.

For elliptical loadings, the present model correlates with that of Maskell and Spence (ref. 1), since it is actually a generalization of their technique, although a slightly different form of the auxiliary equation is used. The proper test of the lifting-line/auxiliary-equation model is the comparison with a properly numerically modeled linearized lifting-surface theory, with the appropriate kinematic and dynamic boundary conditions applied to a wing of zero thickness. The only existing lifting-surface model properly satisfying the wake boundary conditions is that of Lopez and Shen (ref. 9). Reference 9 shows excellent correlation of Maskell and Spence's model with the Lopez and Shen lifting-surface approach. The present model can thus be considered verified for elliptical loading.

The rectangular wing presents a more difficult problem of correlation. Published solutions are given by Tokuda (ref. 8) and Lopez and Shen (ref. 9); these solutions differ by small but significant amounts. As a representation of the differences between the various models, table I shows the ratio of the integrated wing lift to the section lift (C_L/C_ℓ) for a representative design case - elliptical and rectangular wings of aspect ratio 6.0 at the blowing coefficients of 1.0 and 2.0. In obtaining these data, the data from reference 9 was ready from a graph; while for Tokuda's result (ref. 8), his equation 6.6 was used. This equation is read as

$$\frac{C_L}{C_\ell} = \frac{1}{1 + \left[\log_{10}\left(\frac{8A}{C_{\ell_\alpha}}\right) + 1.577\right]\frac{C_{\ell_\alpha}}{4\pi A}} \qquad (71)$$

This form is written out since there is some ambiguity in the enunciation of equation 6.6 in reference 8. As a further baseline, the classical lifting-line unblown $(C_J = 0)$ results of Glauert are shown in the last column. It can be seen that the present paper correlates rather well with the lifting-surface solution while Tokuda's result (ref. 8) is somewhat higher. It can be concluded that the present analysis correlates with the lifting-surface approach at least in this range.

Table I also illustrates that there is about as much variation in solutions between the rectangular and the elliptical planform as there is in the different analytical approaches. While all solutions are probably acceptable for preliminary design purposes, it would be very valuable to have a few known exact solutions to test approximate methods against.

TABLE I.- RATIO OF WING LIFT TO SECTION LIFT FOR 0-PERCENT-THICK ASPECT-RATIO-6 WING

		$C_J = 1.0$	$C_J = 2.0$	$C_J = 0.0$ (from Glauert)
Elliptical Planform	Maskell & Spence ($\sigma = 0.5$)	0.699	0.680	0.751
	Maskell & Spence (correct σ)	.700	.702	
	Kerney	.740	.743	
Rectangular Planform	Tokuda	0.790	0.765	0.720
	Lopez & Shen	.683	Not avail.	
	Lissaman ($\sigma = 0.5$)	.664	.656	
	Lissaman (correct σ)	.675	.668	

The effect of thickness on lift slope is very significant and appears to be larger for the blown wing than a plain wing. Some representative results are shown in table II where the thickness correction of reference 3 is used for the blown elliptical wing, and the present method used for the rectangular wing. In table II, the ratio of $C^t_{L_{p_\alpha}}$ for a 10-percent-thick aspect-ratio-6 wing to $C^o_{L_{p_\alpha}}$ for a 0-percent-thick aspect-ratio-6 wing is presented.

TABLE II.- EFFECT OF THICKNESS ON PRESSURE-LIFT-CURVE SLOPE

Planform	$C^t_{L_{p\alpha}}/C^o_{L_{p\alpha}}$	
	$C_J = 0$	$C_J = 2.0$
Elliptical	1.075	1.100
Rectangular	1.046	1.102

It can be seen from figure 4 that a 10-percent-thick aspect-ratio-6 wing has about the same performance as a 0-percent-thick aspect-ratio-8 wing.

Comparison With Experiment

From the preceding comments, it can be observed that comparison with experiment is a difficult process, largely because few carefully controlled experiments exist. Difficulties in proper normalization of experimental data involve not only the usual problems of viscous boundary-layer effects which occur with all wings, but the special jet-flap problems relating to proper determination of jet coefficient and jet angle, as well as the problem of proper wind-tunnel corrections for a jet-flap wing. In this light, the approximate thickness corrections and the use of an experimental effective aspect ratio can be used to fit a theoretical solution to almost any experimental data.

As an illustration of this point, figure 6 shows a comparison of the present theory with the experimental results of Williams and Alexander reported in reference 11. The curves of the present theory were obtained by directly inserting the given data (namely planform, aspect ratio, thickness, angle of attack, blowing coefficient, and jet angle) into the program with no "corrections". It can be seen that the correlation is very good for lift slope, but that there appears to be a systematic error in the lift at 0° angle of attack. This could be due to the fact that the jet is not actually issuing at its nominal angle of 31.3°. It is of interest to note that after making an approximate global thickness correction, the results of Tokuda (ref. 8) match the experiment even better. However, Maskell

and Spence (ref. 1) match the same data with a similar global thickness correction although their solution is for an elliptical wing with elliptical blowing, giving quite different results for $C_{L_\alpha}/C_{\ell_\alpha}$ as shown in table I.

CONCLUSIONS

An analysis has been developed for high-aspect-ratio jet-flap wings of arbitrary (including discontinuous) geometry and blowing. This analysis has been programed, and the results lead to the following conclusions:

1. The technique is as accurate as other known theoretical methods.

2. The program is more flexible and rapid than other methods, particularly with regard to discontinuities in wing geometry.

3. Correlation with existing experimental data is satisfactory, but it is considered that definitive test data are lacking.

4. The present method is a useful analytical tool for jet-flap wing design.

5. Two additional steps are needed to evaluate jet-flap theories. These theories should be checked against:

   a. Definitive lifting-surface analyses

   b. Properly controlled and corrected experimental tests

Such checks should include cases with variable discontinuous planform and blowing parameters.

APPENDIX A

TREFFTZ PLANE FORCES

GENERAL

Here, the situation in the Trefftz plane where all forces on the wing may be indirectly determined is considered. It is convenient to use the exact nonlinear large angle analysis initially, and then to expand to the appropriate order of accuracy.

UNBLOWN WING

The unblown case is treated first to establish a reliable connection with conventional Trefftz plane theory. It is assumed that a self-preserving steady wake exists in the Trefftz plane (fig. A1). Thus, in places inclined at $\bar{\alpha}$ to the mainstream flow V, the situation is properly two dimensional. Incompressible flow of density ρ is assumed. In this inclined plane, for steady two-dimensional flow, a complex potential $W(z)$ is defined as

$$W = V \sin \bar{\alpha} \, (-iz + w(z)) \tag{A1}$$

where $z = x + iy$ with x horizontal and y upwards in the Trefftz plane. The normalized perturbation potential $w(z)$ may be written

$$w(z) = \phi \, (x,y) + i \, \Psi \, (x,y) \tag{A2}$$

Forces in the direction z and y are now considered by applying the momentum theorem to a large cylinder of axis parallel to the final wake direction.

On the upstream face, velocity and pressure have their free-stream values; on the downstream face, the velocity is $V \cos \bar{\alpha}$ in the direction of the cylinder axis $V \sin \bar{\alpha} \, \phi_x$ in the x (spanwise) direction and $V \sin \bar{\alpha} \, (1 + \phi_y)$

in the orthogonal y direction. Thus the pressure perturbation Δp in the Trefftz plane is given by

$$\Delta p = \frac{1}{2} \rho V^2 \left\{ 1 - \cos^2 \bar{\alpha} - \sin^2 \bar{\alpha} \, (1 + \phi_y)^2 - \sin^2 \bar{\alpha} \, \phi_x{}^2 \right\} \tag{A3}$$

For the forces in the Z direction F_z, there are only pressure contributions giving

$$F_z = -\int_{S_1} \Delta p \, dS^* \tag{A4}$$

where S_1 is the infinite downstream face of the cylinder and dS^* is the elemental surface area, substituting equation (A3) gives

$$2 F_z = \rho V^2 \sin^2 \bar{\alpha} \int_{S_1} \left[2 \phi_y + \phi_y{}^2 + \phi_x{}^2 \right] dS^* \tag{A5}$$

For the y force, only momentum need be considered giving

$$F_y = -\rho V^2 \cos \bar{\alpha} \sin \bar{\alpha} \int_{S_1} \phi_y \, dS^* \tag{A6}$$

Noting that ϕ decays sufficiently rapidly at $x,y \to \infty$, these surface integrals can be converted by Gauss Theorem into line integrals about the wake. Assuming the wake is linear and oriented in the x direction, the symmetries of the upper and lower surfaces of the wake give

$$2 F_z = \rho V^2 \sin^2 \bar{\alpha} \left\{ - 4 \int \phi \, dx - 2 \int \phi \, \phi_y \, dx \right\} \tag{A7}$$

$$F_y = \rho V^2 \cos \bar{\alpha} \sin \alpha \, 2 \int \phi \, dx \tag{A8}$$

where ϕ is the potential and ϕ_y its gradient on the upper surface of the wake.

This can now be resolved into the conventional lift and drag directions to obtain the following exact relations

$$L = \rho V^2 \sin \bar{\alpha} \left\{ 2 \int \phi \, dx + \sin^2 \bar{\alpha} \int \phi \, \phi_y \, dx \right\} \tag{A9}$$

$$D = - \rho V^2 \sin^2 \bar{\alpha} \cos \bar{\alpha} \int \phi \, \phi_y \, dx \tag{A10}$$

For $\bar{\alpha}$ small, these degenerate to the classical linearized results. Results similar to the above are given by Ribner (ref. 12); however, in that version, the induced drag is left in the form of an infinite surface integral, as opposed to the convenient finite line integral given here.

It is now assumed that the trailing vorticity which must satisfy the Beltrami condition, that is, be parallel to the local flow, has negligible lateral (spanwise) components in the wake. Then, each spanwise station in the Trefftz plane contains the same lift as the corresponding spanwise wing station. Thus, defining the local lift coefficient as $C_\ell(x)$ and local chord as c, the following is obtained

$$C_\ell(x) = 4 \sin \bar{\alpha} \, \frac{\left\{ \phi(x) + \frac{\sin^2 \bar{\alpha}}{2} \phi(x) \, \phi_y(x) \right\}}{c} \tag{A11}$$

By making the same assumption for the local induced-drag coefficient $C_d(x)$, the following is obtained

$$C_d(x) = - 2 \sin^2 \bar{\alpha} \cos \bar{\alpha} \, \phi(x) \, \frac{\phi_y(x)}{c} \tag{A12}$$

It should be noted here, that while this result is correct for the lift for any planform, it is only valid for induced drag if the planform is essentially unswept. For swept wings, it is known that the distribution of induced drag in the Trefftz plane does not correspond to that on the wing itself, although the total induced drag, of course, can be obtained by integration either on the wing or in the Trefftz plane.

APPENDIX A

BLOWN CASE

The jet sheet is now introduced assuming the momentum at each station to be $\gamma(x)$ and inclined at an angle $\beta(x)$ to the horizontal (positive downwards). Then

$$\beta = \bar{\alpha} - \tan^{-1}\left\{ \tan \bar{\alpha} \, (1 + \phi_y) \right\} \tag{A13}$$

$$\beta \approx - \bar{\alpha} \, \phi_y + \sigma \, (\bar{\alpha}^3) \tag{A14}$$

Thus, to second order, the additional force coefficients due to the jet element are

$$C_{\ell_j}(x) = - \frac{2 \, \gamma(x) \, \bar{\alpha} \, \phi_y(x)}{c \, \rho \, V^2} \tag{A15}$$

$$C_{dj}(x) = - 2 \, \gamma(x) \, \frac{\left(1 - \frac{\bar{\alpha}^2}{2} \, \phi_y(x)^2\right)}{c \, \rho \, V^2} \tag{A16}$$

Then, writing C_j as the local jet-momentum coefficient with c the local chord

$$C_j = \frac{\gamma}{\left(\frac{1}{2} \, \rho V^2\right)} \tag{A17}$$

for the blown wing gives

$$C_\ell(x) = + \frac{4 \, \bar{\alpha} \, \phi(x)}{c} - C_j \, \bar{\alpha} \, \phi_y(x) + 0 \left(\bar{\alpha}^3\right) \tag{A18}$$

$$C_d(x) = - \frac{2 \, \bar{\alpha}^2 \, \phi(x) \, \phi_y(x)}{c} - C_j \left(1 - \frac{\bar{\alpha}^2 \, \phi_y(x)^2}{dc}\right) + 0 \left(\bar{\alpha}^4\right) \tag{A19}$$

APPENDIX A

It is shown in equation (A19) that the terms without C_j account for the vortex lift both on the wing and in the jet wake.

The force contribution due to the entire jet sheet can now be computed directly by considering conditions at the trailing edge of the wing. Assuming the wing to be uncambered, with the local geometrical angle of attack to be $\alpha(x)$ and with the jet angle relative to the wing to be $\theta(x)$, the direct momentum force is subtracted to obtain the pressure components on the wing itself in coefficient form as

$$C_{\ell_p} = + \frac{4\,\bar{\alpha}\,\phi}{c} - C_j \left(\bar{\alpha}\,\phi_y + \alpha + \theta\right) \tag{A20}$$

$$C_{d_p} = - \frac{2\,\bar{\alpha}\,\phi\,\phi_y}{c} + \frac{1}{2} C_j \left\{\bar{\alpha}^2\,\phi_y{}^2 - \left(\alpha + \theta\right)^2\right\} \tag{A21}$$

These are now resolved relative to the chordline to give the normal force coefficient C_n and the thrust coefficient C_t. To second order in $\bar{\alpha}$ and α, these become

$$C_n = + \frac{4\,\bar{\alpha}\,\phi}{c} - C_j \left(\bar{\alpha}\,\phi_y + \alpha + \theta\right) \tag{A22}$$

$$C_t = \frac{4\,\bar{\alpha}\,\phi}{c} \left(\alpha + \frac{\bar{\alpha}\,\phi_y}{2}\right) + \frac{C_j}{2} \left\{\theta^2 \left(\alpha + \bar{\alpha}\,\phi_y\right)^2\right\} \tag{A23}$$

This pair constitutes the outer solution, expressing the pressure forces on the wing itself.

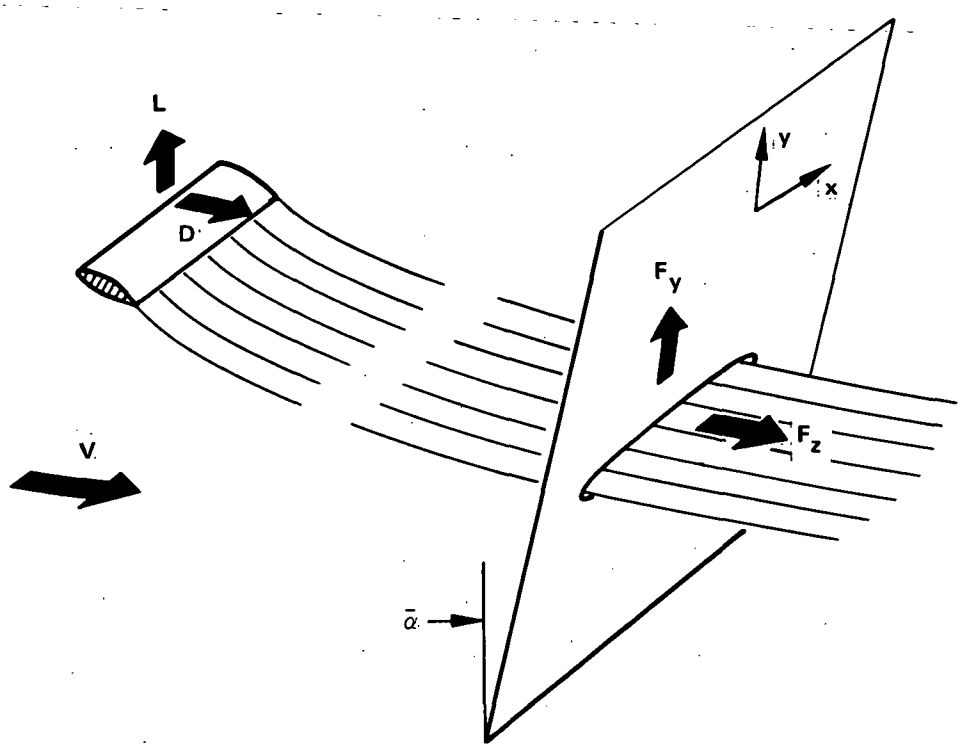

FIGURE A1. GEOMETRY OF TREFFTZ PLANE

APPENDIX B

JET-FLAP THICKNESS CORRECTION

GENERAL

The analytical results for jet-flap performance used in the paper are for the linearized problem; that is: the airfoil thickness is linearized; the position of the jet wake is assumed to be on the airfoil chordline; and the dynamic boundary condition itself is linearized. To find the first order effects of linearization, an exact nonlinear solution is assumed to be known for a Joukowski airfoil, and they by a mapping to an auxiliary plane. This is reduced to a flat-plate airfoil. Then, by expanding the mapping to appropriate order, the ratio of the lift in the two planes can be determined, assuming that the lift on the flat airfoil in the auxiliary plane is given with sufficient accuracy by linearized theory. The analysis is two dimensional and incompressible.

ANALYSIS

Figure B1 shows a thick Joukowski airfoil and the auxiliary airfoil and defines the symbols used. The potential in the physical plane, $Z = X + i\,Y$ given by $W(Z) = \Phi + i\,\Psi$, is assumed. Q is the complex conjugate velocity dW/dz.

The boundary conditions are as follows:

$$\text{kinematic:}\quad \Psi = 0 \quad \text{on airfoil and wake} \tag{B1}$$

$$\text{dynamic:}\quad \left[\left(Q^{+}\right)^2 - \left(Q^{-}\right)^2\right] = \frac{C\,C_j\,Q_\infty^{\,2}}{R} \tag{B2}$$

where $+$ and $-$ refer to upper and lower surfaces of the vortex wake, C the chord, C_j the momentum coefficient, and R the radius of curvature of the wake.

This geometry is now assumed to be mapped to the auxiliary $z' = x + i\,y$ plane by

APPENDIX B

$$z' = F(Z) \ , \ dz'/dZ = f^* \tag{B3}$$

where under f^* the airfoil maps to a slit. Potential is conserved at corresponding points. The mapping is required to have the following properties:

$$f^* \to 1 \ , \ Z \to \infty \tag{B4}$$

$$f^* \text{ regular at } T' \tag{B5}$$

$$f^* \text{ analytical elsewhere except at } N \tag{B6}$$

where T' is the trailing edge of the airfoil and N the leading edge. It should be noted that corresponding elements are given by

$$dz' = f^* \, dZ \tag{B7}$$

so that the length and angle of an element in each plane are given by

$$ds = |f^*| \, dS \ , \ \theta^* = (\arg f^*) + \Theta^* \tag{B8}$$

with

$$dz' = ds \, \theta^{i\theta^*} \ , \ dZ = dZ \, \phi^{i\theta^*} \tag{B9}$$

Under this mapping, the boundary conditions become

kinematic: $\Psi = 0$ on body and wake

$$\text{dynamic: } \left[\left(q^+\right)^2 - \left(q^-\right)^2 \right] = c' \, q_\infty{}^2 \, \frac{C}{C'} \, \frac{C_j}{f^*} \left\{ 1 - \frac{d}{d\theta^*} (\arg f^*) \right\} \frac{d\theta^*}{ds} \text{ .. on wake} \tag{B10}$$

where θ^* is the inclination of the wake in the auxiliary plane; ds an arc length along the wake in the plane; and q the complex conjugate velocity in this plane.

Thus, this now becomes a nonlinear problem of flow about a jet flapped flat plate of chord c' at angle α with jet angle of θ and with a momentum coefficient c_j which varied according to

$$c_j = \frac{C}{c'} \frac{C_j}{f^*} \left\{ 1 - \frac{d}{d\theta^*} (\arg f^*) \right\} \tag{B11}$$

THE MAPPING FUNCTION

The parametric functional relationships can be expressed as

$$Z = \mu + \frac{1}{\mu} \tag{B12}$$

$$z' = \mu + a + \frac{(1 + a)^2}{\mu + a} \tag{B13}$$

where μ is an intermediate complex parameter. This transforms the Joukowski airfoil to the flat plate, with the required properties on the derivative. In addition, the following geometric properties are noted

	Z Plane	z' Plane
Chord	$\equiv \frac{4 + 4 a^2}{1 + 2 a} = C$	$4 (1 + a) = c'$
Thickness	$\equiv \frac{4 a}{1 + a} = T$	$0 = t$

The mapping derivative

$$f^* = \frac{dz}{d\mu} \cdot \frac{d\mu}{dZ} \tag{B14}$$

is evaluated as

$$f^* = \left\{1 - \frac{\left(1 + 2a + a^2\right)\left(1 + \frac{a}{\mu}\right)^{-2}}{\mu^2}\right\}\left\{\frac{\mu^2}{\mu^2 - 1}\right\} \tag{B15}$$

$$\sim 1 - 2a\,\frac{1}{\mu(\mu + 1)} - \frac{a^2}{\mu^2} + O\left(a^3\right) \tag{B16}$$

At the trailing edge

$$f^* \sim 1 - a - a^2 \tag{B17}$$

while downstream

$$f^* \to 1 \tag{B18}$$

The approach to unity is very rapid. For example at $\mu = 3$, which is about 0.5-chord length downstream, it can be found that $f^* \simeq 0.98$ for a 10-percent-thick airfoil.

EQUIVALENT PROBLEM

Thus, the equivalent problem consists of finding the exact solution in the z plane of the flow about a flat plate of chord $c' = 4(1 + a)$ immersed in a distance flow of velocity q_∞ and angle α and having a jet flap of variable strength. This strength is given by equation (B11), substituting equation (B16) and expanding to O(a) gives

$$c_j \simeq \frac{c}{c'}\,\frac{C_j}{1 - a} \quad \text{at the trailing edge} \tag{B19}$$

$$c_j = \frac{c}{c'}\,C_j \quad \text{at infinity} \tag{B20}$$

APPENDIX B

Substituting for

$$C = \frac{4\,(1 + a^2)}{(1 + 2\,a)} \tag{B21}$$

and expanding to $O(a)$ gives

$$c_{j1} \simeq \frac{C_j}{(1 - a^2)} \quad \text{at the trailing edge} \tag{B22}$$

$$c_j = \frac{C_j}{(1 - a)} \quad \text{at infinity} \tag{B23}$$

The pressure field on the airfoil is now assumed to be a function of the blowing coefficient c_{j1} at the trailing edge. Then, using standard linearized theory, γ_a is the circulation about the airfoil alone and is given by

$$\frac{2\,\gamma_a}{C} = \left(C^o_{\ell_\alpha}\,\alpha + C^o_{\ell_\theta}\,\theta\right) - \left(\alpha + \theta\right) c_{j1} \tag{B24}$$

where $C^o_{\ell_\alpha}$ and $C^o_{\ell_\theta}$ are the lift slopes for 0 thickness computed for a blowing coefficient of c_{j1}.

Spence (ref. 2) gives

$$C^o_{\ell_\alpha} = 2\left(\pi\,c_{j1}\right)^{1/2}\left(1 + O\left(c_{j1}\right)\right)^{1/2} \tag{B25}$$

but

$$c_{j1} = C_j\left(1 + a^2 + O\left(a^2\right)\right) \simeq C_j\left(1 + O\left(a^2\right)\right) \tag{B26}$$

So $c_{jl} = C_j$ near the trailing edge, giving

$$\frac{2\gamma_a}{C} = C_\ell^o - (\alpha + \theta)\, C_j \tag{B27}$$

since

$$C_\ell^o = C_{\ell_\alpha}^o\, \alpha + C_{\ell_\theta}\, \theta \tag{B28}$$

Under the mapping, $Z \to z$, potential is conserved so tha circulation about the thick airfoil in the physical Z plane, Γ_a, is given by

$$2\,\Gamma_a = C\left\{C_\ell^o - (\alpha + \theta)\, C_j\right\} \tag{B29}$$

However, the wake lift in the physical Z plane is given by

$$(\alpha + \theta)\, C_j\, C \tag{B30}$$

Thus, the total circulation in the physical plane is given by

$$2\,\Gamma = C\left(C_\ell^o - (\alpha + \theta)\, C_j\, C\right) + \left(\alpha + \theta\right) C_j\, C \tag{B31}$$

So that the lift coefficient in the physical plane is given by

$$C_\ell^t = \frac{c'}{C}\left\{C_\ell^o + \left(\alpha + \theta\right) C_j \left(\frac{C}{c'} - 1\right)\right\} = \left(1 + a\right)\left\{C_\ell^o - \left(\alpha + \theta\right) C_j \frac{a}{1 + a}\right\} \tag{B32}$$

noting that

$$\frac{c'}{C} = 1 + a + O(a^2) \tag{B33}$$

APPENDIX B

Noting that the mapping gives

$$\frac{T}{C} = \frac{a}{1+a} \cdot \frac{1+2a}{1+a^2} \tag{B34}$$

it can be shown that

$$a = \frac{T}{C} + O\left\{\left(\frac{T}{C}\right)^2\right\} \tag{B35}$$

This gives the result to $O(T/C)$ where T/C is the thickness to chord ratio

$$\frac{C_\ell^t}{C_\ell^o} = 1 + \frac{T}{C}\left\{1 - \frac{C_j\,(\alpha+\theta)}{C_\ell^o}\right\} \tag{B36}$$

Thus, in physical terms, it is observed that the thickness affects only that portion of the lift directly experienced on the airfoil (the pressure lift). This result was intuitively proposed as a correction by Spence. The above analysis, while still an approximation, provides a rationale for this correction.

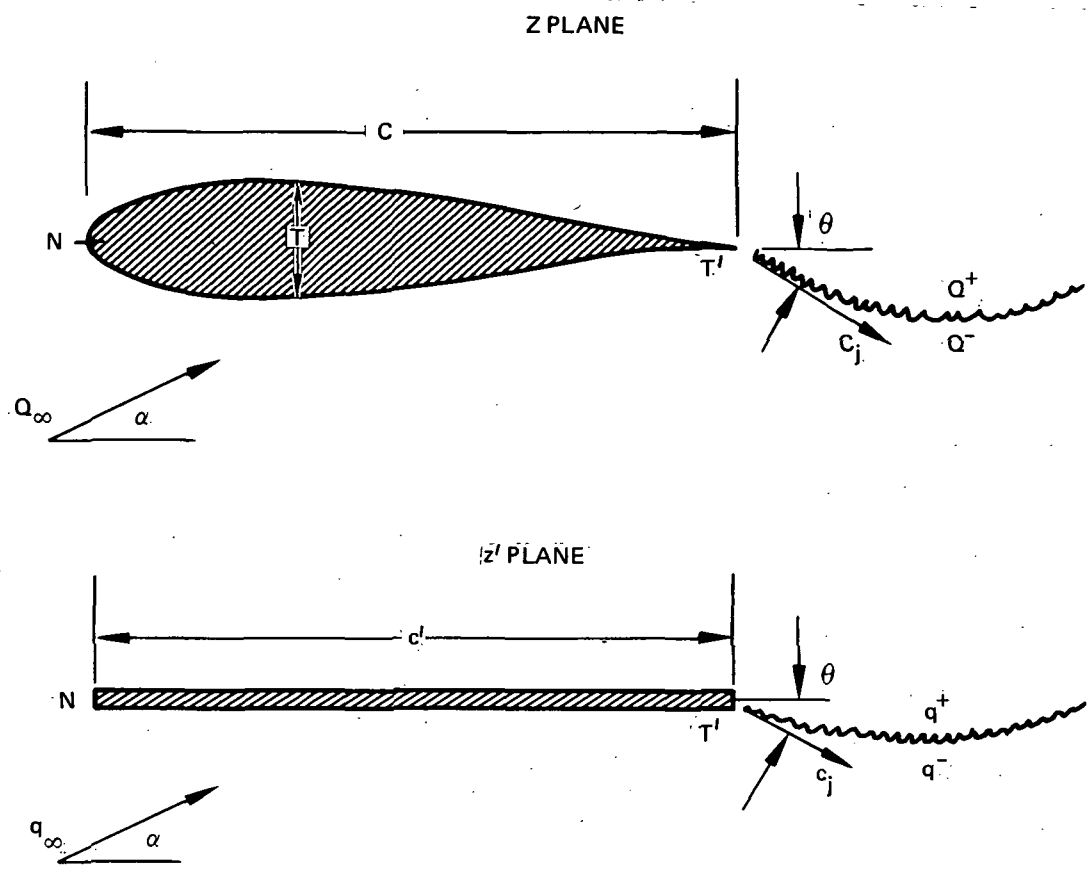

FIGURE B1. PHYSICAL AND AUXILIARY AIRFOIL PLANES

REFERENCES

1. Maskell, E. C.; and Spence, D. A.: A Theory of the Jet Flap in Three Dimensions. Proc. Roy. Soc. (London), ser. A, vol. 251, no. 1266, June 9, 1959, pp. 407-425.

2. Spence, D. A.: The Lift Coefficient of a Thin, Jet-Flapped Wing. Proc. Roy. Soc. (London), ser. A, vol. 238, no. 1212, Dec. 4, 1956, pp. 46-48.

3. Spence, D. A.: The Lift Coefficient of a Thin Jet-Flapped Wing. II. A Solution of the Integro-Differential Equation for the Slope of the Jet. Proc. Roy. Soc. (London), ser. A, vol. 261, no. 1304, April 11, 1961, pp. 97-118.

4. Spence, D. A.: The Lift on a Thin Aerofoil With a Jet Augmented Flap. Aeronaut. Quart., vol. 9, pt. 3, Aug. 1958, pp. 287-299.

5. Lissaman, P. B. S.: A Linear Theory for the Jet Flap in Ground Effect. AIAA J., vol. 6, no. 7, July 1968, pp. 1356-1362.

6. Kuchemann, D.: A Method of Calculating the Pressure Distribution Over Jet Flapped Wings. R. & M. No. 3036, Brit. A.R.C., 1957 .

7. Kerney, K. P.: A Theory of the High Aspect Ratio Jet Flap. AIAA J., vol. 9, no. 3, Mar. 1971, pp. 431-435.

8. Tokuda, N.: An Asymptotic Theory of the Jet Flap in Three Dimensions. J. Fluid Mech., vol. 46, pt. 4, Apr. 27, 1971, pp. 705-726.

9. Lopez, M. L.; and Shen, C. C.: Recent Developments in Jet Flap Theory and Its Application to STOL Aerodynamic Analysis. AIAA Paper No. 71-578, 1971.

10. Multhopp, H.: The Calculation of the Lift Distribution of Aerofoils. R.T.P. Translation No. 2392, British M.A.P.

11. Williams, J.; and Alexander, A. J.: Three-Dimensional Wind-Tunnel Tests of a 30° Jet Flap Model. C.P. No. 304, Brit. A.R.C., 1957.

12. Ribner, H. S.: On the Lift and Induced Drag Associated With Large Downwash Angles. UTIA Tech. Note No. 19, Univ. of Toronto, Inst, Aerophysics, Jan. 1958.

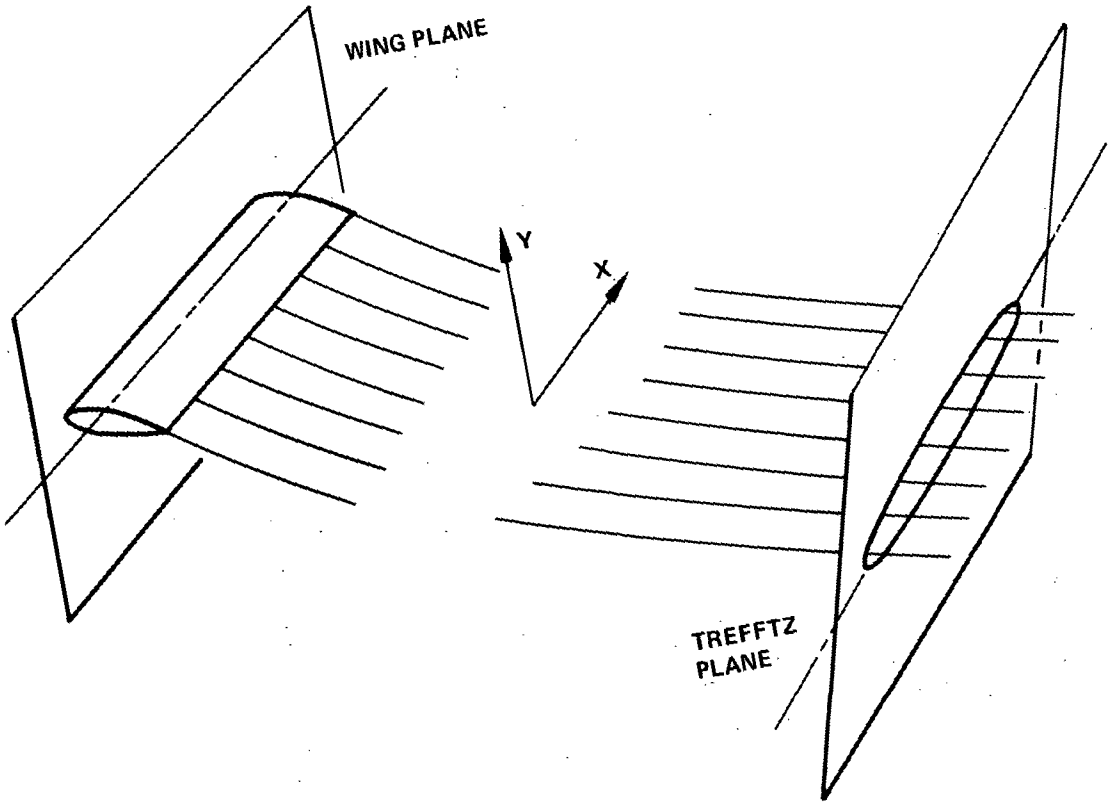

FIGURE 1. GEOMETRY OF SPANWISE PLANES

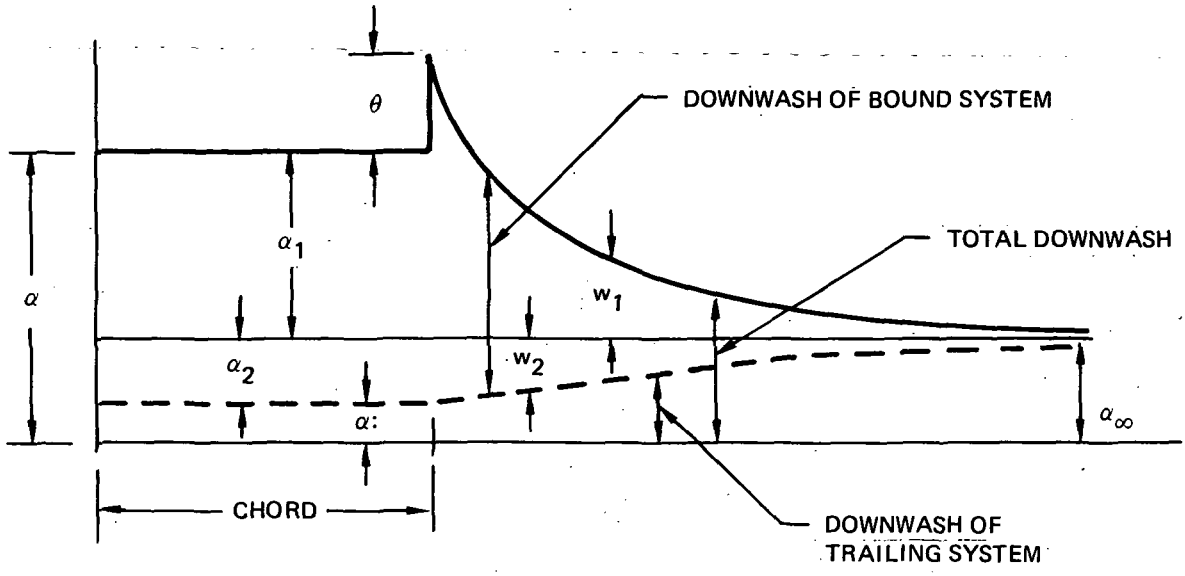

FIGURE 2. CHORDWISE DOWNWASH OF JET FLAP WING

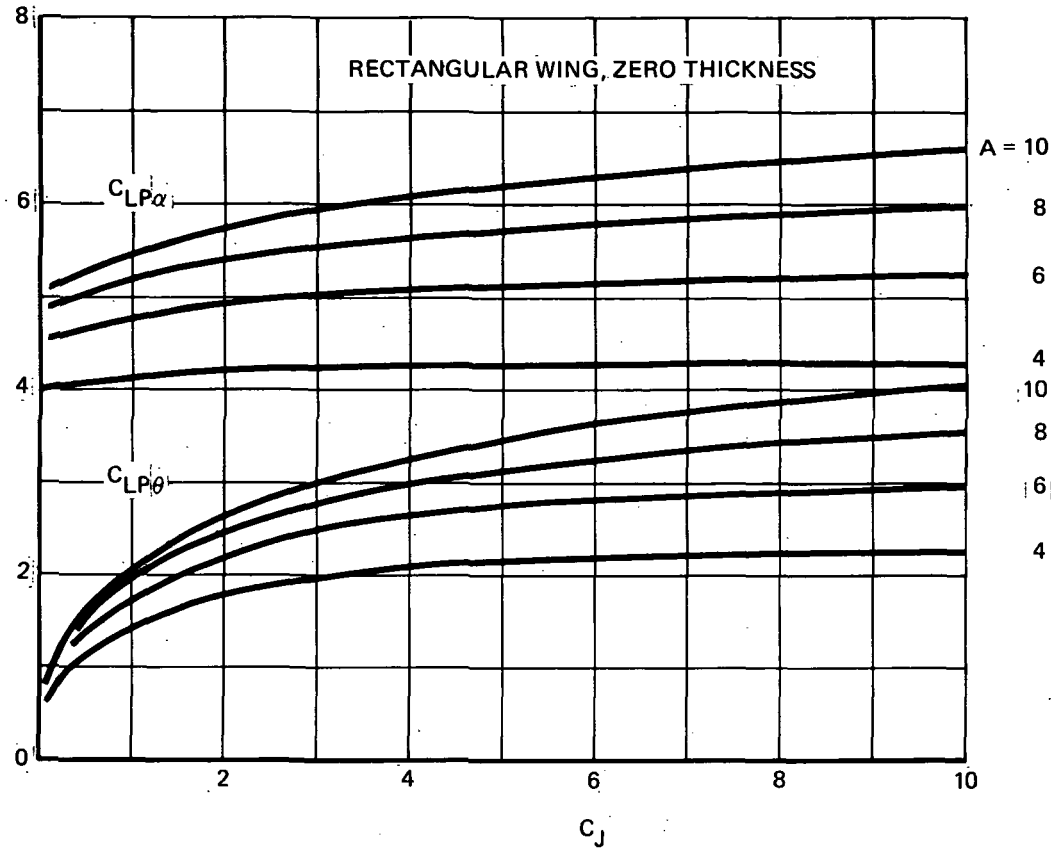

FIGURE 3. PRESSURE LIFT GRADIENTS FOR RECTANGULAR WING OF ZERO THICKNESS

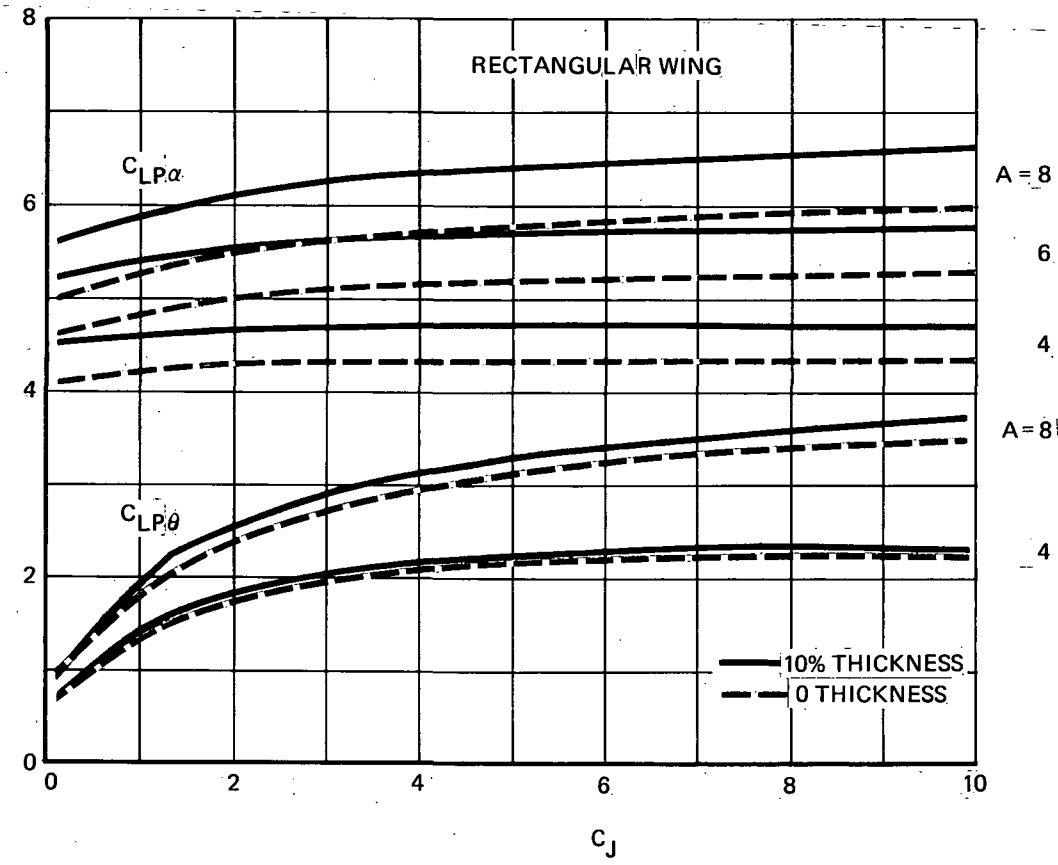

FIGURE 4. PRESSURE LIFT GRADIENTS FOR RECTANGULAR WING OF FINITE THICKNESS

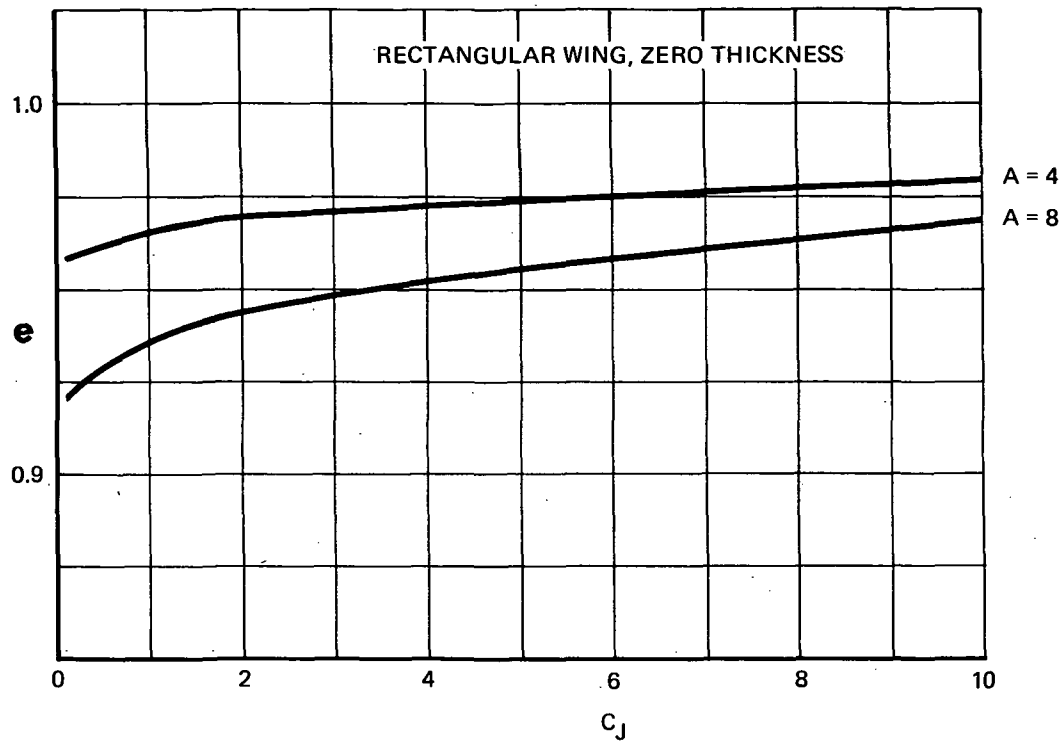

FIGURE 5. INDUCED DRAG EFFICIENCY FOR RECTANGULAR WINGS

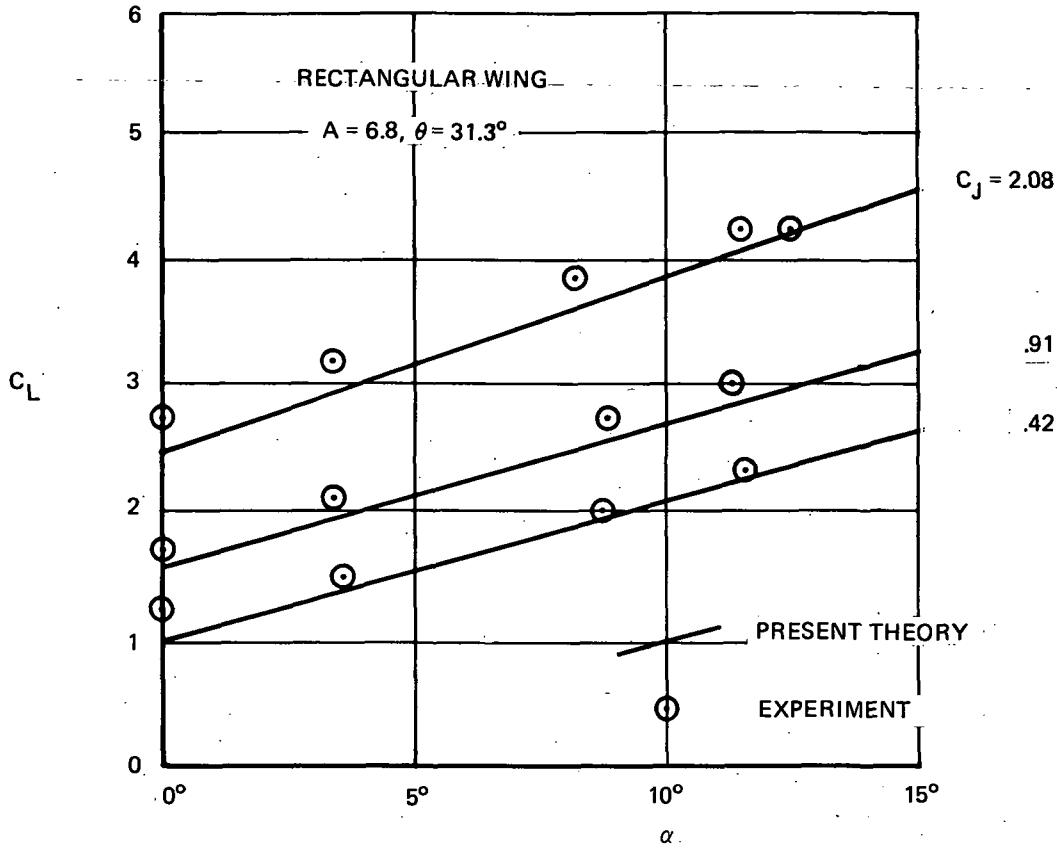

FIGURE 6. COMPARISON OF THEORY WITH EXPERIMENT

"The aeronautical and space activities of the United States shall be conducted so as to contribute . . . to the expansion of human knowledge of phenomena in the atmosphere and space. The Administration shall provide for the widest practicable and appropriate dissemination of information concerning its activities and the results thereof."

—NATIONAL AERONAUTICS AND SPACE ACT OF 1958

NASA SCIENTIFIC AND TECHNICAL PUBLICATIONS

TECHNICAL REPORTS: Scientific and technical information considered important, complete, and a lasting contribution to existing knowledge.

TECHNICAL NOTES: Information less broad in scope but nevertheless of importance as a contribution to existing knowledge.

TECHNICAL MEMORANDUMS: Information receiving limited distribution because of preliminary data, security classification, or other reasons. Also includes conference proceedings with either limited or unlimited distribution.

CONTRACTOR REPORTS: Scientific and technical information generated under a NASA contract or grant and considered an important contribution to existing knowledge.

TECHNICAL TRANSLATIONS: Information published in a foreign language considered to merit NASA distribution in English.

SPECIAL PUBLICATIONS: Information derived from or of value to NASA activities. Publications include final reports of major projects, monographs, data compilations, handbooks, sourcebooks, and special bibliographies.

TECHNOLOGY UTILIZATION PUBLICATIONS: Information on technology used by NASA that may be of particular interest in commercial and other non-aerospace applications. Publications include Tech Briefs, Technology Utilization Reports and Technology Surveys.

Details on the availability of these publications may be obtained from:

SCIENTIFIC AND TECHNICAL INFORMATION OFFICE

NATIONAL AERONAUTICS AND SPACE ADMINISTRATION

Washington, D.C. 20546